Verification of large-scale rapid transport in the lower thermosphere: Tracking the exhaust plume of STS-107 from launch to the Antarctic

R. Niciejewski,[1] W. Skinner,[1] M. Cooper,[1] A. Marshall,[1] R. R. Meier,[2] M. H. Stevens,[3] D. Ortland,[4] and Q. Wu[5]

Received 10 November 2010; accepted 12 January 2011; published 4 May 2011.

[1] New analysis of the Doppler shift of O_2 airglow spectra recorded by the TIMED Doppler Interferometer (TIDI) and the High Resolution Doppler Imager (HRDI) have provided conclusive evidence that the shuttle main engine exhaust plume generated in the lower thermosphere by the launch of STS-107 and imaged by the Global Ultraviolet Imager (GUVI) instrument on TIMED was transported to the Antarctic in ~80 h, supporting a key inference from the initial study by Stevens et al. (2005). These new results were aided by improved knowledge of the effects of instrumental and satellite artifacts imposed on the Doppler spectra. STS-107 launched on 16 January 2003, and the neutral wind near its launch trajectory and nearby volume was sampled within minutes by TIDI. These initial observations suggested that the northernmost end of the shuttle's exhaust plume would move northeast and that the southern end would move southeast, motions that were identified in imagery acquired during the next orbit of TIMED. The direction and magnitude of plume motion inferred from GUVI images obtained 12, 26, and 50 h after launch were again confirmed by TIDI and HRDI. The appearance of the plume over the Antarctic ~80 h after launch, inferred from earlier work by the appearance of iron ablated from the shuttle's main engines, was consistent with neutral winds measured by the satellite Doppler instruments over the Antarctic. The transport of the plume from the coast of Florida to the Antarctic was aided by the favorable phase and strong amplitude of a 2 day planetary wave of wave number three in the southern hemisphere on 18 January 2003. The existence of the 2 day wave was deduced from zonally averaged and combined TIDI and HRDI neutral wind observations. We conclude that the existence of strong and sustained winds in the MLT, significantly greater than expected from empirical and theoretical models, is indisputable and provides compelling evidence supporting the global-scale nature of thermospheric winds with magnitude greater than 100 m/s observed by Larsen (2002) from 40 years of sounding rocket chemical release experiments.

Citation: Niciejewski, R., W. Skinner, M. Cooper, A. Marshall, R. R. Meier, M. H. Stevens, D. Ortland, and Q. Wu (2011), Verification of large-scale rapid transport in the lower thermosphere: Tracking the exhaust plume of STS-107 from launch to the Antarctic, *J. Geophys. Res.*, *116*, A05302, doi:10.1029/2010JA016277.

1. Introduction

[2] It is well known that the dynamics of the mesosphere and lower thermosphere (MLT) regions of the upper atmosphere can be dominated by tides. Solar heating of water vapor in the troposphere and ozone in the stratosphere excite vertically propagating diurnal and semidiurnal tides. Horizontal structure is determined by large-scale circulation, which is driven by the spatial variation of solar heating. The rotation of the Earth imparts a westward motion that forms global tidal oscillations. These migrating diurnal and semidiurnal tides are relatively easy to observe in resolved meridional and zonal MLT winds [*Niciejewski and Killeen*, 1995; *Fisher et al.*, 2002]. Seasonal variations of in situ excitation at lower altitudes generate upward propagating disturbances with transient characteristics that are much more difficult to detect in MLT horizontal winds. Planetary waves impart multiple day periodicities [*Wu et al.*, 1993, 1994] on global-scale winds, while gravity waves can influence winds locally over short time periods through temperature perturbations [*Meriwether and Gerrard*, 2004]. The degree by which migrating tides in the MLT covary with planetary

[1]Space Physics Research Laboratory, University of Michigan, Ann Arbor, Michigan, USA.
[2]Department of Physics and Astronomy, George Mason University, Fairfax, Virginia, USA.
[3]Space Science Division, Naval Research Laboratory, Washington, D. C., USA.
[4]NorthWest Research Associates, Bellevue, Washington, USA.
[5]National Center for Atmospheric Research,Boulder, Colorado, USA.

0148-0227/11/2010JA016277

waves and gravity waves continues to provide a significant source of uncertainty in fully understanding the dynamics of the MLT.

[3] Observations of winds in the MLT continue to elicit contentious interpretations. *Larsen* [2002] summarizes the results of 40 years of chemical release experiments. The chemical tracers were released along either or both the ascending and descending trajectories of sounding rockets. When the evolution of these bright tracers was observed by a suite of ground-based cameras and the position of the trail triangulated against background stars, the components of the MLT horizontal wind were obtained. Many individual altitude profiles contain measurements of large wind magnitude over short vertical scales that in the context of any single rocket launch suggest outlier points. *Larsen* [2002] has digitized all 400 available data sets into a compendium and performed simple statistical analyses to highlight the fact that maximum winds greater than 100 m/s in the MLT occur at a frequency of 60%. Direct comparisons with reference dynamic models such as the Horizontal Wind Model (HWM) [*Hedin et al.*, 1991] were unsuccessful in predicting such strong individual winds.

[4] Most radio frequency and lidar techniques that monitor the neutral wind in the MLT require spatial and temporal averaging. These comprise the bulk of the "raw" data that have been used to generate spectral functions for the HWM. A relatively new and highly sensitive method to measure the neutral wind in the MLT employs nonspecular echoes [*Oppenheim et al.*, 2009] detected by incoherent scatter radar. Unlike traditional meteor radars that employ the specular echo from meteor trails to measure the line of sight Doppler velocity of the neutral wind, plasma irregularities generated by the meteor are the source for this new technique. Echoes recorded by different sections of the radar receiver exhibit a phase difference related to the position of the meteor trail, and tracking the phase difference over time while the trail remains in the radar beam provides an estimate of the neutral horizontal wind. Without the inherent averaging necessary with classical meteor radars, velocities in excess of 100 m/s are observed in the MLT with vertical shears reminiscent of sounding rocket profiles at high spatial and temporal resolution. Large winds have also been observed using a sodium lidar with altitude profiles that are comparable to chemical release wind profiles [*Larsen and Fesen*, 2009].

[5] Since 1981, the space shuttle has been an important transportation system between Earth and space. To date, over 130 flights have been made through the MLT. The general impact of powered flight through the MLT has been of interest since *Kellogg* [1964] presented calculations related to anthropogenic effects on the upper atmosphere. The main conclusion was that even though the MLT is considered tenuous, other than with a few exceptions, it would require thousands of large rocket launches annually to impact the worldwide natural budget of CO_2, NO, or water vapor in the MLT.

[6] Large effects can also be found in the ionosphere, where water vapor releases such as the aptly named WATERHOLE experiment have been extensively used to study diffusion and plasma depletion effects at 300 km altitude [*Mendillo et al.*, 1980; *Yau et al.*, 1981]. In the latter, charge exchange with atomic oxygen ions rapidly ionized water vapor, which then quickly recombined with free electrons effectively generating a depletion zone in the vicinity of the release. *Kellogg* [1964] provided estimates related to the effects that prevailing winds and diffusion might have on rocket exhaust at various altitude regimes: in the lower thermosphere above the turbopause, molecular diffusion dominates and will thoroughly mix the exhaust plume with the ambient atmosphere in ~1 week. As diffusive mixing transports a contaminant to lower altitudes, turbulent mixing becomes more important in distributing the plume components in the mesosphere and stratosphere.

[7] Recent interest in the effects of powered flight through the upper atmosphere has been highlighted by coincidental increases in the occurrence frequency of polar mesospheric clouds from the main engine exhaust of the space shuttle [*Kelley et al.*, 2010]. As described in a continuing series of articles, there have been several unexpected observations of shuttle exhaust plumes at locations distant from the launch site off the Florida coast. STS-66, launched on 3 November 1994, carried onboard instrumentation to measure the global distribution of hydroxyl airglow and surprisingly observed the hydroxyl signature of its own launch in the Arctic 1 day into the mission [*Stevens et al.*, 2002]. The mean meridional speed inferred from the measurements was as high as 40 m/s northward. STS-85, launched on 7 August 1997, flew the same aeronomy payload and again observed the hydroxyl signature of its exhaust plume [*Stevens et al.*, 2003] beginning the day after launch inferring a northward speed of 35 m/s. Coincident ground based microwave spectrometer observations from Andenes Norway confirmed the presence of water vapor in volumes common to the hydroxyl enhancements observed from the shuttle. Five days later, assuming that water vapor descended at a constant speed of 5 cm/s, enhanced solar scattering from newly formed high latitude clouds at altitudes near 82 km was observed from the shuttle and attributed to its own launch exhaust plume. *Stevens et al.* [2005] later showed that one shuttle plume contributed 22% of the total water ice mass over one PMC season.

[8] Water vapor emission associated with the exhaust plumes of STS-112 and STS-113 in 2002 was observed by the SABER (Sounding of the Atmosphere using Broadband Emission Radiometry) experiment on the TIMED (Thermosphere Ionosphere Mesosphere, Energetics and Dynamics) satellite [*Siskind et al.*, 2003]. These observations showed that the exhaust plumes traveled several thousand kilometers from where they were released implying mean meridional speeds as high as 60 m/s southward. The launch plume of STS-107, launched 16 January 2003, provided a strong signature that was viewed 2 days after launch off the southwest coast of South America [*Stevens et al.*, 2005]. A day and a half later, above Rothera Research Station on the Antarctic Peninsula, an iron lidar observed an echo above 100 km that was probably due to iron ablated from the shuttle's main engines. The frequency of mesospheric clouds increased dramatically in the days following this event, the burst representing 10–20% of the observed ice mass for the season. This suggested a sustained southward meridional speed of 44 m/s. *Kelley et al.* [2010] observed intense noctilucent clouds in the Arctic several days following the 8 August 2007 launch of STS-118.

[9] The rapid transport of shuttle exhaust over exceptionally long distances implies a high and sustained mean meridional speed in the MLT. The extremely sensitive STS-85 hydroxyl observations suggest a long life to the plume and

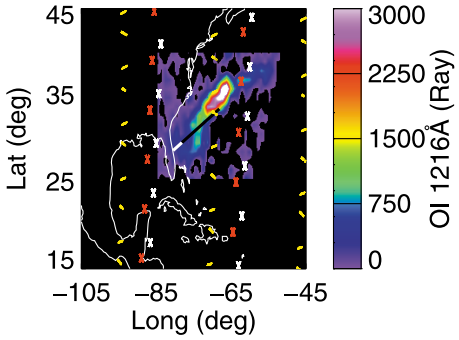

Figure 1. Mosaic combining the Lyman-α brightness of the shuttle plume obtained by GUVI ~105 min after STS-107 MECO with the geo-located positions of altitude scans by the TIDI cold-side telescopes (red, white crosses) and SABER (yellow). The ground track of the ascent of STS-107 is shown with white representing altitudes < 100 km and black representing altitudes > 100 km. The track terminates at MECO, ~500 s after launch (1539:00 UT on 16 January 2003).

rapid expansion of the water vapor cloud. *Kelley et al.* [2009] argue that these features are anomalies, cannot be explained classically, and are the result of two-dimensional turbulent flow above the turbopause. *Meier et al.* [2010], however, argue that ordinary molecular diffusion, dominating above the turbopause where the exhaust is placed initially, is the natural explanation for the expansion of atomic hydrogen in the plume. *Kelley et al.* [2009] also argue that their proposed turbulent flow can account for the anomalously fast horizontal transport.

[10] The present paper presents a detailed and exhaustive summary of correlative Doppler shift measurements of MLT winds obtained in and near the presumed path of the exhaust plume of STS-107 implying that an ordinary 2 day planetary wave is responsible for a large part and perhaps all of the observed travel. This simple correlation between a planetary wave and a shuttle plume has never before been performed and has been facilitated by significant improvements in the instrumental characterization of the spaceborne instrumentation.

[11] Multiplicity in observation strategies for viewing MLT winds may either be a prerequisite for intensive campaigns or the result of good fortune. This study falls into the latter category. On 16 January 2003, shuttle STS-107 was launched beneath the TIMED satellite, orbiting at an altitude of 625 km. In the lower thermosphere, as the main engines of the shuttle burned through the liquid oxygen and liquid hydrogen fuel, a 300 t water vapor plume was created that was viewed by three TIMED instruments within minutes of launch and for several days following launch. During a typical shuttle launch, the main engines operate for approximately 8 1/2 min. The shuttle ascends for the first 4 min reaching an altitude of 100 km when it is roughly 200 km downrange. The remainder of powered flight is along a horizontal arc between 100 and 115 km altitude extending for another 1000 km downrange. The GUVI (Global UltraViolet Imager) instrument acquired H Lyman-α imagery of the shuttle plume against the disc of the Earth, describing the geographical location and horizontal spread of the exhaust. The SABER instrument viewed altitude profiles of emission products of the plume. The TIDI (TIMED Doppler Interferometer) instrument observed altitude profiles of the Doppler shift of O_2 airglow, which when correlated with GUVI and SABER sightings of the shuttle plume, documented the horizontal neutral wind in and around the exhaust trail. Additional Doppler shift measurements of O_2 dayglow provided by HRDI (High Resolution Doppler Imager) flying aboard UARS (Upper Atmospheric Research Satellite) measured the horizontal wind in the MLT at different local solar times for plume positions inferred from GUVI. Finally, supporting evidence from several ground-based radars describing the dynamical nature of the MLT along the path that the shuttle exhaust plume was presumed to take was located in a publication by *Pancheva et al.* [2006].

2. Observations

2.1. Less Than 2 h After Launch

[12] The STS-107 space shuttle mission was launched at 1539:00 UT on 16 January 2003. The STS-107 mission was the last shuttle flight that did not dock with the International Space Station or the Hubble Space Telescope and thus orbited the Earth at a lower inclination angle of 39 degrees resulting in a more easterly ascent than a typical station mission. An unplanned overflight of the shuttle ascent was performed by TIMED on orbit 5998. TIMED was flying backward, ascending northward, with its cold side pointed toward the shuttle launch plume, which was visible on the Earth's limb. Figure 1 displays a mosaic of a GUVI image and symbols marking tangent limb intercepts for TIDI and SABER lines of sight along with the ground track of the powered portion of the STS-107 ascent. The GUVI disc image was acquired during orbit 5999 (one orbit later) as TIMED flew over the long-lived space shuttle plume. The statistical uncertainty of the binned pixels is between 100 and 200 Rayleighs, somewhat less than *Stevens et al.* [2005] as the bin sizes are different. This GUVI channel transmits the hydrogen Lyman-α spectral feature, which is produced directly by resonantly scattered sunlight as well as by secondary scattering from atomic hydrogen emission in the thermosphere. In this nadir directed view, extant Lyman-α dayglow has been removed from the raw image leaving a bright trail nearly parallel with the powered launch path of STS-107 (white below 100 km altitude, black above 100km). The source of the atomic hydrogen in the bright trail is shuttle exhaust in the form of both atomic hydrogen and H produced via photodissociation of the water vapor exhaust product by sunlight [*Hicks et al.*, 1999; *Meier et al.*, 2010].

[13] GUVI recorded the shuttle plume at ~1732 UT as indicated in GUVI Level 1C, v003r00 data, or ~105 min after MECO. The TIMED Level hierarchy (1B, 1C, 2, etc.) refers to data products that have undergone increasingly more sophisticated analysis. In that short time, the trail had been twisted away from its initial trajectory by lower thermospheric winds. The altitude distributions of the shuttle exhaust plume radiances were measured by SABER approximately 6 min after MECO and are illustrated in Figure 2. The SABER noise levels in the observed channels are indicated by the NER or noise equivalent radiance [*Tansock et al.*, 2003]. The limb tangent location, 32.7°N and 69.0°W, intersected the flight path of STS-107 as shown in Figure 1. Signifi-

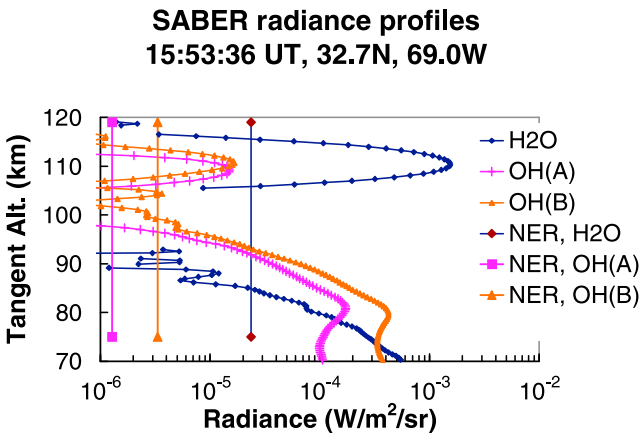

Figure 2. SABER observations of H_2O (blue) and OH (red, violet) radiance acquired at 1553:36 UT on 16 January 2003 intersecting the shuttle plume at 32.7°N, 69.0°W.

cant responses as indicated in SABER Level 1B, version 01.07 data were seen with a FWHM of ~5 km in both the H_2O channel at 6.9μ and the two OH channels (A centered at ~2.0μ recording the Meinel (9,7) and (8,6) bands, B centered at ~1.6μ recording the Meinel (5,3) and (4,2) bands) in the neighborhood of 110 km. The peak water radiance was a factor of 4 greater than the strongest response reported by *Siskind et al.* [2003] for shuttle launches in 2002 and is equivalent to the atmospheric emission at 60 km altitude. The hydroxyl signature of the shuttle plume is the first Meinel band emission of a shuttle plume recorded by SABER. Shuttle plume hydroxyl emission had previously been observed at 308 nm by MAHRSI aboard STS-66 [*Stevens et al.*, 2002]. The slight separation in the peak altitudes of the two different OH Meinel wavelengths has previously been reported in the literature [*Winick et al.*, 2009]. Hydroxyl is the other principal by-product from the photodissociation of water by sunlight, mentioned above as a mechanism for atomic hydrogen production from shuttle exhaust.

[14] The two TIDI cold-side telescopes observed the limb at tangent locations identified by the red and white crosses in Figure 1. Horizontally resolved wind profiles are shown in Figure 3 for orbit 5998, corresponding to samples along the 64W meridian in Figure 1 for the period encompassing the launch of STS-107. Positive meridional wind is to the north, and positive zonal wind is to the east. The components of the neutral wind were determined from the nearest pairs of inverted line of sight wind profiles using Level 2, version 10 TIDI data, measured with the O_2 At (0,0) P9 doublet. The tangent intercepts displayed in Figure 1 refer to the averaged location of each vertical P9 scan over the altitude range 70 to 115 km, the components of which would have a spread similar to that shown for SABER. The cadence of P9 scans does not reflect all of the observations performed by TIDI during a scan: not shown are P15 observations, OI (5577Å) observations, and dark count samples. The statistical uncertainties of the zonal and the meridional wind profiles acquired at 24.9°N latitude are shown and are representative of dayside data acquired prior to cleaning maneuvers performed on 28 January 2003. These operations resulted in a sevenfold improvement in TIDI sensitivity to airglow emissions and a considerable reduction in the statistical wind uncertainty.

[15] The basic production analysis for TIDI used to arrive at the data in Figure 3 was described by *Niciejewski et al.* [2006]. Since that publication, significant improvements have been made in the TIDI data products, most importantly, (1) a greatly improved background level and airglow continuum model, and (2) a time-dependent "zero-wind" model. The time dependency assumes the zero wind is the sum of a daily mean value and a track angle dependent cosine term which is due to the change in the earth rotation component in the line of sight and solar heating variations of the instrument baseplate along the orbit. The sensitivity of TIDI permits it to unintentionally record on/off cycles of various satellite control units: in particular, in 2005 TIMED converted its attitude determination from onboard gyroscopes to star-tracking cameras reducing its power dissipation by 60 Watts. TIDI recorded this event as a 50 m/s change in line of sight drift, requiring an improved and time-dependent instrumental drift description. This sensitivity is also evident during 4 out of 6 of each year's 60 day beta or yaw cycles. In all cases, it is not the etalon that exhibits a temperature related shift but folding mirrors and perhaps telescopes at the entrance end of TIDI. Statistical studies of multiple years of TIDI airglow fringes have produced the improvements that are incorporated into Version 10 products. Work continues to cross-validate the O_2 At P9 winds with coincident O_2 At P15 and OI (5577Å) winds and shall be the subject of a future publication.

[16] Figure 1 suggests that at the point of MECO the shuttle plume has been twisted to the northeast, while near the point at which STS-107 reached 100 km altitude (white-to-black

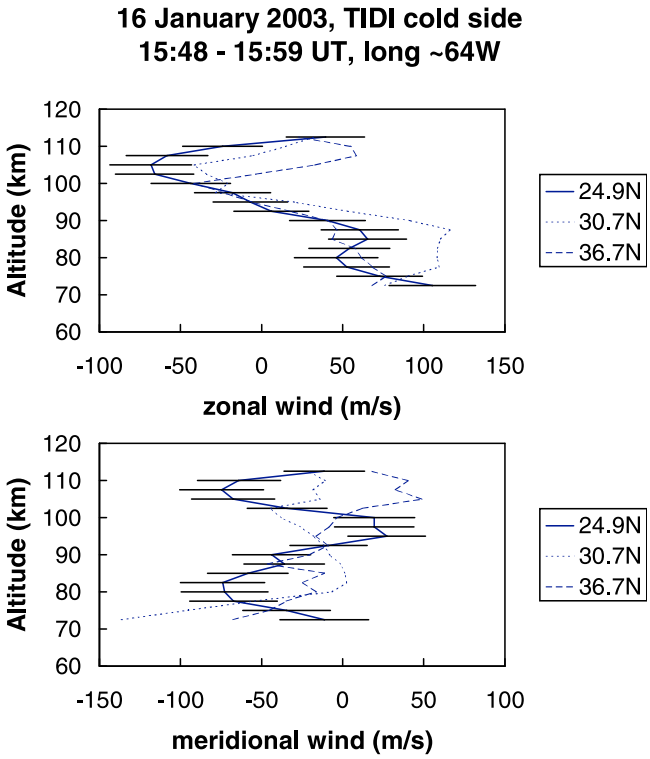

Figure 3. Altitude profiles of the resolved horizontal neutral winds observed by TIDI to the east of the shuttle ascent, within minutes of MECO. The (top) zonal component is positive eastward and the (bottom) meridional component is positive northward.

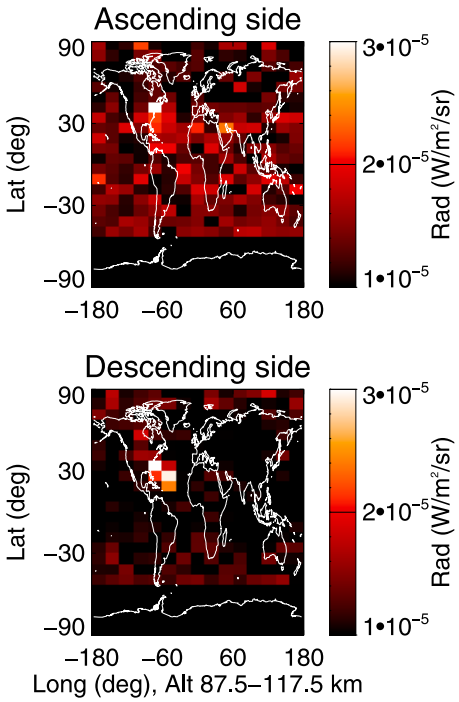

Figure 4. SABER H_2O brightness integrated over the altitude range 87.5–117.5 km on 17 January 2003 geo-located in 15 longitude bins (~1 per orbit) and 7.5 degree latitude bins (~1 scan). The shuttle plume, off the coast of Florida, is sampled 12 h after launch by SABER at night during the descending part of a TIMED orbit and 24 h after launch, in daylight, during the ascending orbit half.

interface in the ground track), the Lyman-α signature has moved to the southeast closest to the launch site in a short period of time. Lyman-α is absorbed by molecular oxygen below ~85 km [*Hicks et al.*, 1999] and thus cannot be traced back directly to main engine ignition which occurs on the ground. The behavior of the drifts in the shuttle plume suggests a shear in the winds above 100 km. In fact, TIDI data indicate the existence of such a shear along 64W during the launch time frame: the meridional wind at 36.7°N was directed toward the north above 100 km, but changed direction toward the south at 30.7°N and 24.9°N. Assuming that the injection of exhaust by STS-107 into a trail terminated at MECO (~34°N) and the northern end of the plume in the GUVI image located at 37.5°N are related, the northward speed of the plume tip was 44 m/s, essentially matching that measured by TIDI at 110 km altitude at 36.7°N. The southward end of the GUVI plume, though more difficult to identify with specific ground track coordinates other than being near the point where STS-107 ascended above 100 km (the white/black interface on the ground track) does suggest a southward motion, as suggested by the meridional wind measurement at 30.7°N. The eastward zonal speed inferred from the GUVI image for the MECO endpoint was 28 m/s, which was near that observed by TIDI at 36.7°N.

2.2. Twelve Hours After Launch

[17] The 6.9μ channel of SABER transmits emission from transitions within the fundamental ν_2 band of H_2O centered at 6.3μ. The interpretation of this feature has provided water vapor abundance profiles of the stratosphere and mesosphere for both day and night, as observed from space by many instruments for several decades. Nocturnal signatures of rocket exhaust plumes for 2002, including those from the space shuttle, have also been observed by SABER and are summarized by *Siskind et al.* [2003]. Included in their summary is a midinfrared signature of STS-113 recorded 14.6 h after launch. It is clear that SABER is a sensitive instrument for detecting rocket exhaust plumes and that an exhaust plume remains visible for an extended period.

[18] Figure 4 was constructed using a subset of all H_2O data observed by SABER on 17 January 2003. SABER views the tangent limb from the cold side of TIMED, the ascending orbit portions observed primarily during the day and the descending half predominantly at night. TIMED was flying in an orientation that permitted the cold side to view as far north as the pole, but precluded SABER from observing the Antarctic. This situation reverses every 60 day beta cycle. The radiances collected over the altitude range 87.5–117.5 km were coadded, averaged and then binned over a grid with resolution 24 degrees longitude (1 orbit) by 7.5 degrees latitude (one altitude scan): at these altitudes, SABER is noise-limited when attempting to detect natural H_2O 6.3 μ emission. The color coding points to multiple water vapor detections in the neighborhood of the launch ground track and the post-launch GUVI image, which indicates the continued presence of shuttle exhaust.

[19] The SABER water detection on the descending flight path is somewhat misleading in Figure 4 as the sampled longitude is at the seam between two grid points at 60°W, and contributes to adjacent bins. TIMED is located to the west of the SABER limb intercept during the descending path. Figure 5 summarizes all H_2O detections by SABER of the STS-107 plume. The thick black solid line is an average of 6 water profiles acquired over the latitude range 20.8°N to

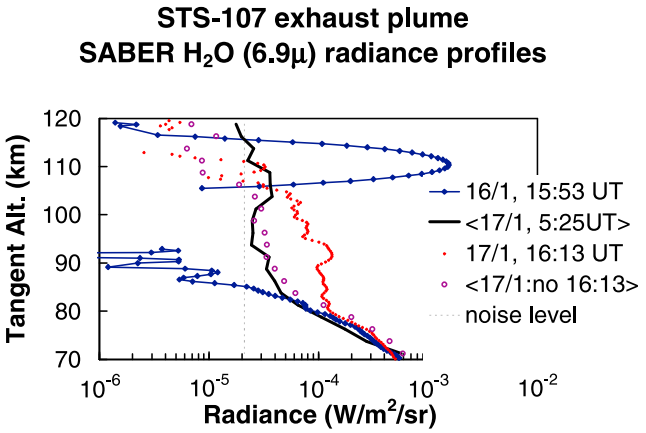

Figure 5. Summary of the SABER H_2O observations of the STS-107 exhaust trail. The green trace represents the plume observed within minutes of MECO. The thick black trace is the average of all plume scans observed 12 h after launch. The red trace corresponds to the most intense single scan acquired 24 h after launch, while the large dots define the average of the remaining plume measurements also sampled 24 h after launch. The noise level for a single H_2O scan, 2.1 W/m^2/sr is shown.

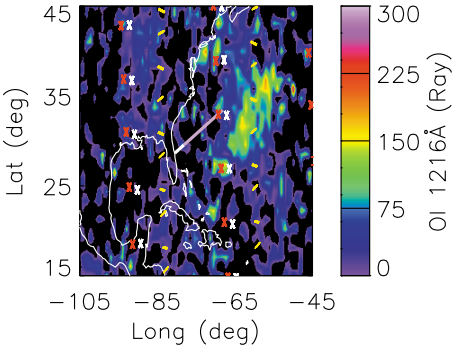

Figure 6. A mosaic of four nightside Lyman-α scans obtained by GUVI 12 h after launch, corrected for background brightness. The shuttle plume appears to the east of the magenta ground track of STS-107. The positions of TIDI scans are shown as red and white crosses, and SABER scans appear in yellow.

38.4°N over a span of ~5 min centered at 0525 UT that contribute to the descending path water detections.

[20] The STS-107 Lyman-α plume persisted into the night. This can be seen in Figure 6, which displays a background-corrected mosaic of four GUVI Lyman-α disc images (i.e., images from four successive orbits) centered on the STS-107 launch ground track; the format is similar to Figure 1. The nightglow background transmitted by GUVI is negligible compared to the dayglow background, resulting in a statistical uncertainty of ~50 Rayleighs in Figure 6. The shuttle plume was recorded primarily in orbit 6005 at ~0345 UT. Though TIMED was viewing the night side, Lyman-α resonant fluorescence from atomic hydrogen continued to show the signature of shuttle exhaust above the background airglow. The initial source of Lyman-α was likely multiple scattering from geocoronal nightglow, itself produced by multiple scattering of dayside hydrogen emission into the Earth's shadow as discussed by *Hicks et al.* [1999]. Even though H was not produced via water photolysis at night, there was sufficient daytime production to maintain a plume, albeit with about 80% less hydrogen. The apparent descent of ~5 km in the peak altitude of H_2O brightness may either be real or result from the plume being in the foreground or background of the line of sight tangent path viewed by SABER. Examination of Figure 6 is inconclusive and suggests both explanations may contribute to the SABER observations. The nightside observation by GUVI of an exhaust plume is not unique as *Hicks et al.* [1999] report one instance of a nocturnal photometric observation by OGO-4 of Lyman-α associated with a rocket exhaust.

[21] TIDI sampled the MLT region on either side of the plume as indicated in Figure 6, along the 44°W meridian between 0339 and 0352 UT and along the 68°W meridian between 0517 and 0531 UT. During night transits, TIDI restricts altitude coverage of the molecular oxygen Atmospheric band to the range 80–105 km. In Figure 7, the northernmost samples of zonal wind at the highest altitudes reported by TIDI indicate an eastward component to the

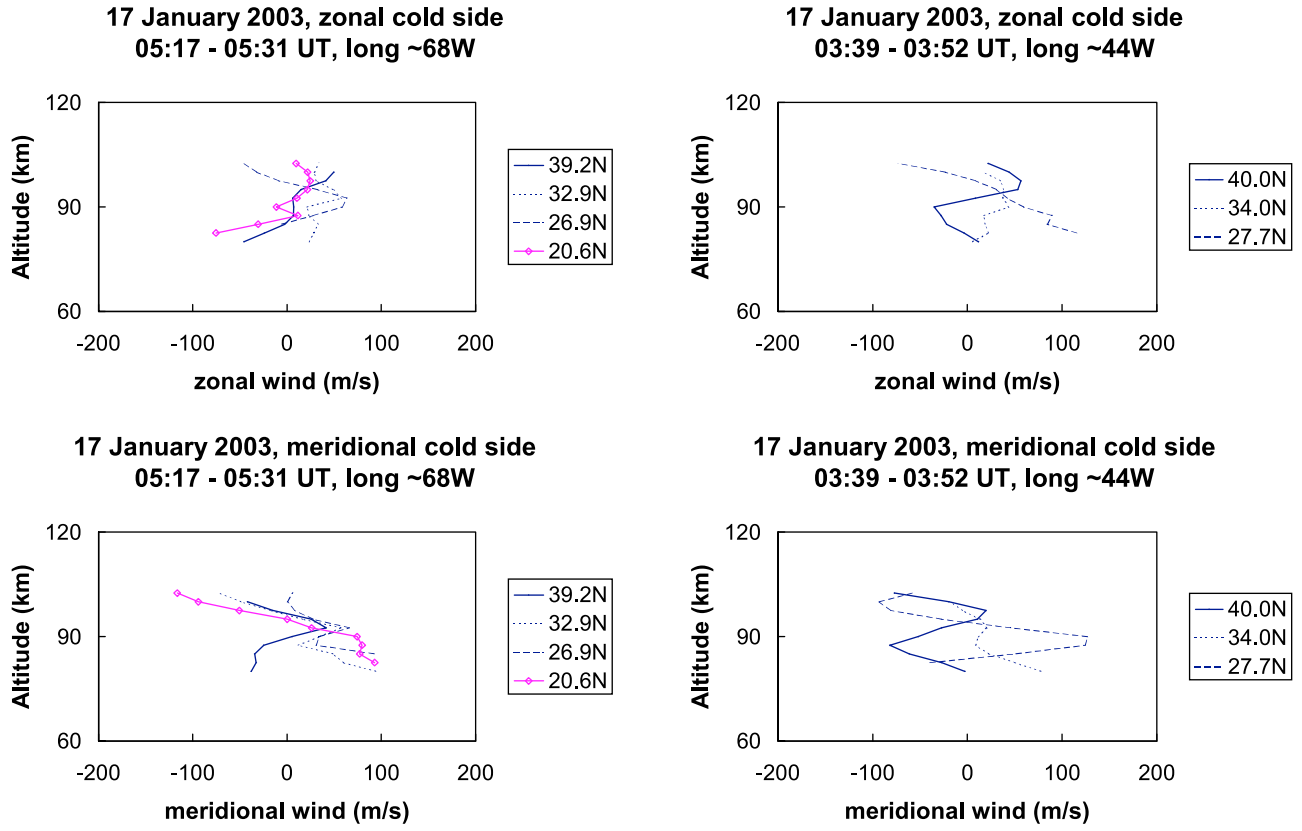

Figure 7. Altitude profiles of the horizontally resolved neutral wind components obtained on both sides of the nightside shuttle plume, (left) 68°W and (right) 44°W. (top) Zonal winds and (bottom) meridional winds. Observations were performed at night over a narrow altitude range.

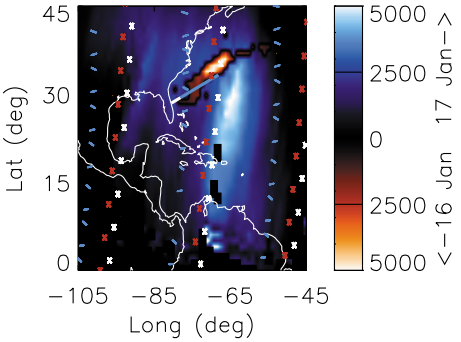

Figure 8. Collage of two GUVI image sets: blue combines scans of the shuttle plume 24 h after launch, while red contains the original plume observation on 16 January 2003. The red and white crosses represent TIDI scans obtained on 17 January 2003, while the light blue lines represent SABER.

horizontal wind, supporting the easterly motion inferred from the GUVI imagery of the presumed MECO northern endpoint. Assuming that the brightest image response corresponds to the MECO endpoint, then the change in longitude was ~8.5 degrees (773 km) requiring a constant zonal drift speed of 21 m/s east, very similar to that measured by TIDI at 40°N, 44°W, and 102.5 km. The meridional winds corresponding to highest altitudes and northernmost samples, indicate either an equatorward component or stagnant flow at plume latitudes. Error bars, representative of the statistical uncertainty of nightside wind profiles, are shown for the zonal profile corresponding to 39.2°N latitude in Figure 7.

2.3. Twenty-Six Hours After Launch

[22] The degree of plume expansion and transport can be seen in the superposition of GUVI daytime images from 16 and 17 January. In Figure 8, red is the same image of Figure 1, orbit 5999, while the blue shading contains Lyman-α imagery from orbits 6012 to 6015 acquired on 17 January 2003. The brightest features at 30°N and 65°–70°W, were recorded at ~1610 UT. The tangent limb locations of TIDI sampling (red and white crosses) and SABER sampling (blue lines) are included. The images indicate a spreading of the shuttle exhaust from the previous day toward the northwest of the launch ground track and toward the south.

[23] The ascending portion of Figure 4 defines the location of SABER observations of the day-old shuttle plume. The brightest signal in Figure 4 is in the bin 37.5°–45°N, at launch longitude. This corresponds to the H_2O profile acquired at 1613 UT in Figure 5 at coordinates 40.2°N and 76.6°W. In Figure 8, TIMED would be located to the east and could very likely be viewing water vapor in the foreground as well as at 110 km. The average of four other profiles acquired between latitudes 30.9° and 44.0°N along the 77°W meridian is also shown in Figure 5. The retrieved H_2O signal in this averaged profile is above the noise level for altitudes below 105 km, indicating the presence of shuttle plume water either at the tangent altitudes noted or along the path viewed from TIMED orbiting at ~625 km altitude and ~4 degrees latitude south and ~26 degrees longitude away.

[24] TIDI sampled along the 40°N latitude circle during 3 consecutive orbits and the resolved horizontal winds are displayed in Figure 9. At 100 km, zonal winds are westward, while the meridional flow is approximately zero. At 105 km, the zonal flow continues to be westward at 69° and 94°W longitude, while the meridional flow has a northerly component. These observations at presumed plume altitudes support the general motion of the northern end of the shuttle plume inferred from GUVI Lyman-α images.

[25] Figure 10 displays resolved horizontal winds along two cuts through the shuttle plume: 72°W on the left and 48°W on the right, the former acquired between 1606 and 1616 UT and the latter recorded between 1431 and 1438 UT (one orbit earlier). The latitudes sampled range from the equator to slightly poleward of 30°N and provide a snapshot of the MLT winds in the vicinity of the southward extent of the shuttle plume. Along the 72°W meridian that intersects the plume and between the altitude range 90 to 105 km, the meridional wind is southward reaching peak winds exceeding 100 m/s. The meridional flow is shifted somewhat northward along the 48°W meridian indicating a longitudinal gradient in the neutral MLT wind that could imply zonal structure to the wind field. Zonal winds observed by TIDI are mixed and appear to average to zero keeping the southward plume motion contained within a narrow longitudinal range. The measurements by TIDI support the inferred motion of the southern end of the shuttle plume between the 0345 and 1610 UT images: a 100 m/s meridional drift translates to ~3 degrees of latitude per hour.

2.4. Fifty Hours After Launch

[26] GUVI next imaged the shuttle plume approximately 50 h after launch as shown in the mosaic of Figure 11.

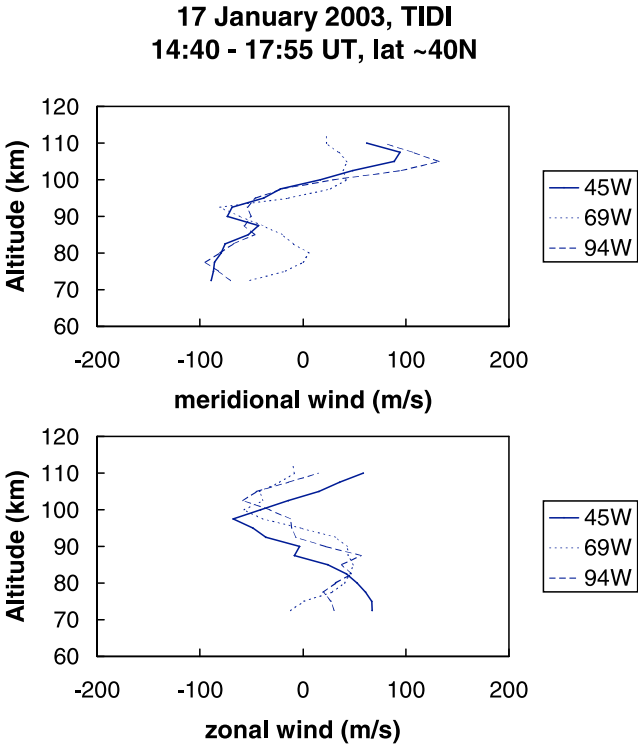

Figure 9. TIDI altitude profiles obtained on 17 January 2003 on three consecutive orbits at ~40°N latitude describing the dynamical environment at the northernmost end of the plume. (top) Meridional winds and (bottom) zonal winds.

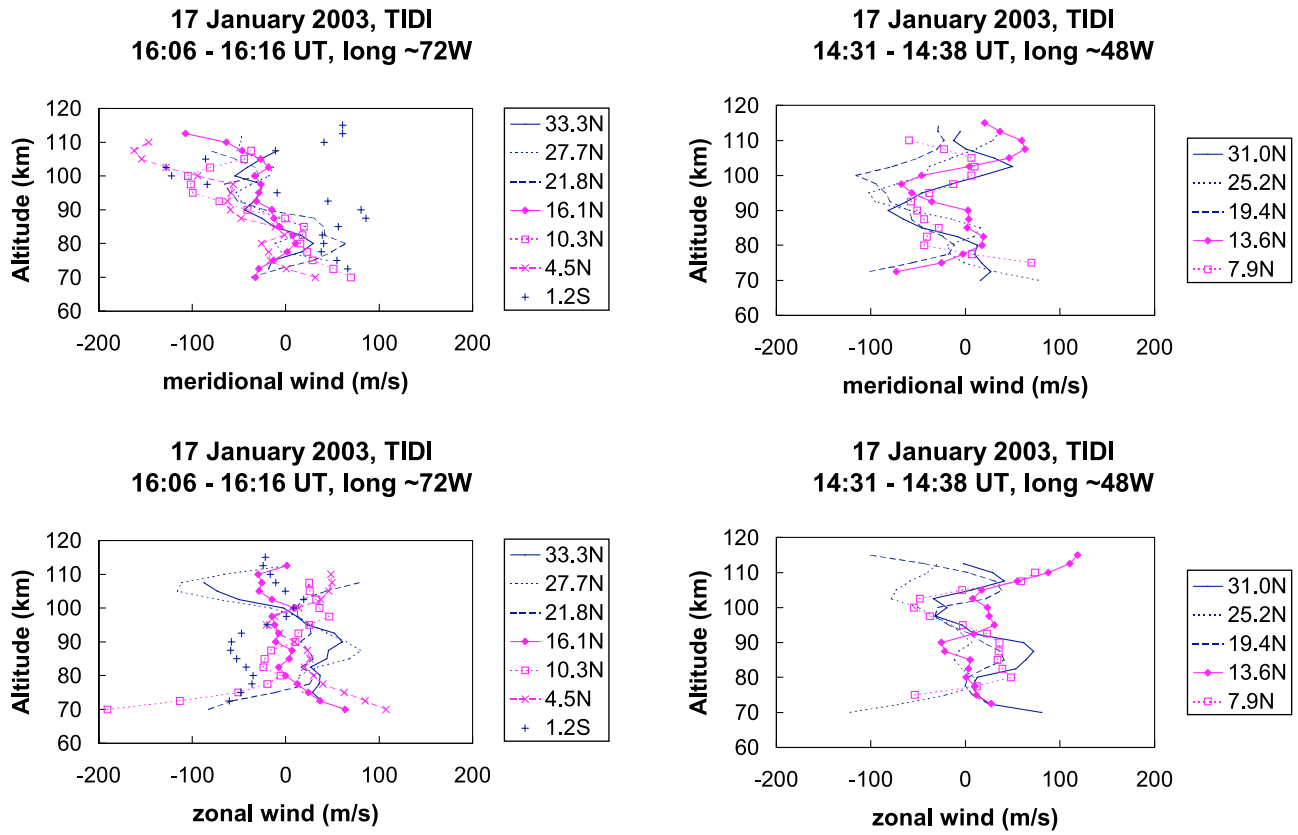

Figure 10. TIDI scans through the southern extension of the shuttle plume at (left) 72°W and to the east of the plume at (right) 48°W recorded on 17 January 2003.

Background airglow corrected Lyman-α images from orbits 6026 to 6030 continue to display a signature of excess hydrogen emission over the latitude range 25°–45°S roughly spread over a 60 degree wide swath south of launch longitude. The brightest features were recorded during orbit 6027 at ~1612 UT. *Stevens et al.* [2005] previously employed the GUVI imagery in Figures 1, 8, and 11 to support arguments for rapid transport of shuttle exhaust to the Antarctic. The inferred motion of the southern limit of the shuttle plume between Figures 8 and 11 suggests approximately 45 degrees southward progression (~5000 km) in a 24 h period, or nearly 60 m/s sustained average speed.

[27] TIDI did not acquire airglow data on 18 January 2003 as operations were devoted to engineering tests. The HRDI instrument, flying aboard UARS, did collect measurements of the MLT wind field on that date. *Skinner et al.* [2003] provide a summary of the operational aspects and issues related to UARS and HRDI for the timeframe relevant to the STS-107 launch, particularly the steps taken to recover HRDI telescope pointing accuracy following the loss of both UARS star trackers. Good attitude knowledge, approaching 0.01°, which is equivalent to a wind error of 1 m/s, for HRDI, now exists for the entire data set encompassing the period 2 November 1991, the date of the first useful scientific measurement, to 31 March 2005, the date of the last HRDI observation before UARS was decommissioned.

[28] The tangent limb coordinates of HRDI data records have been geo-located and categorized by Universal Time in Figure 12, displayed over the longitudinal range of interest. A definite periodicity in real-time contacts with UARS is evident over the four dates shown, reflecting both the slow precession of UARS (~5 degrees westward per day) and the coverage provided by TDRSS for UARS. Most of the points displayed in Figure 12 correspond to dayside altitude scans by HRDI, though some relate to nightside measurements with the telescope commanded to dwell at a nominal altitude of 95 km, e.g., at 0201 UT on 17 January 2003 at latitude 40°S, longitude 69°W. Typically, the measurement density appears as "pairs" corresponding to separate up and down acquisitions in a cycle before the telescope slews to a different azimuth. Nominal operations used a mode where the cold side

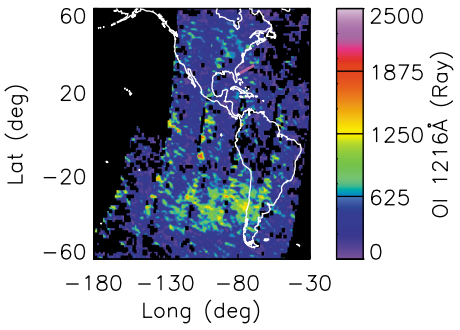

Figure 11. The Lyman-α signature of the STS-107 plume recorded on 18 January 2003, 48 h after launch. The brightest remnant of the shuttle plume is located between 25° and 45°S latitude and 120° and 60°W longitude.

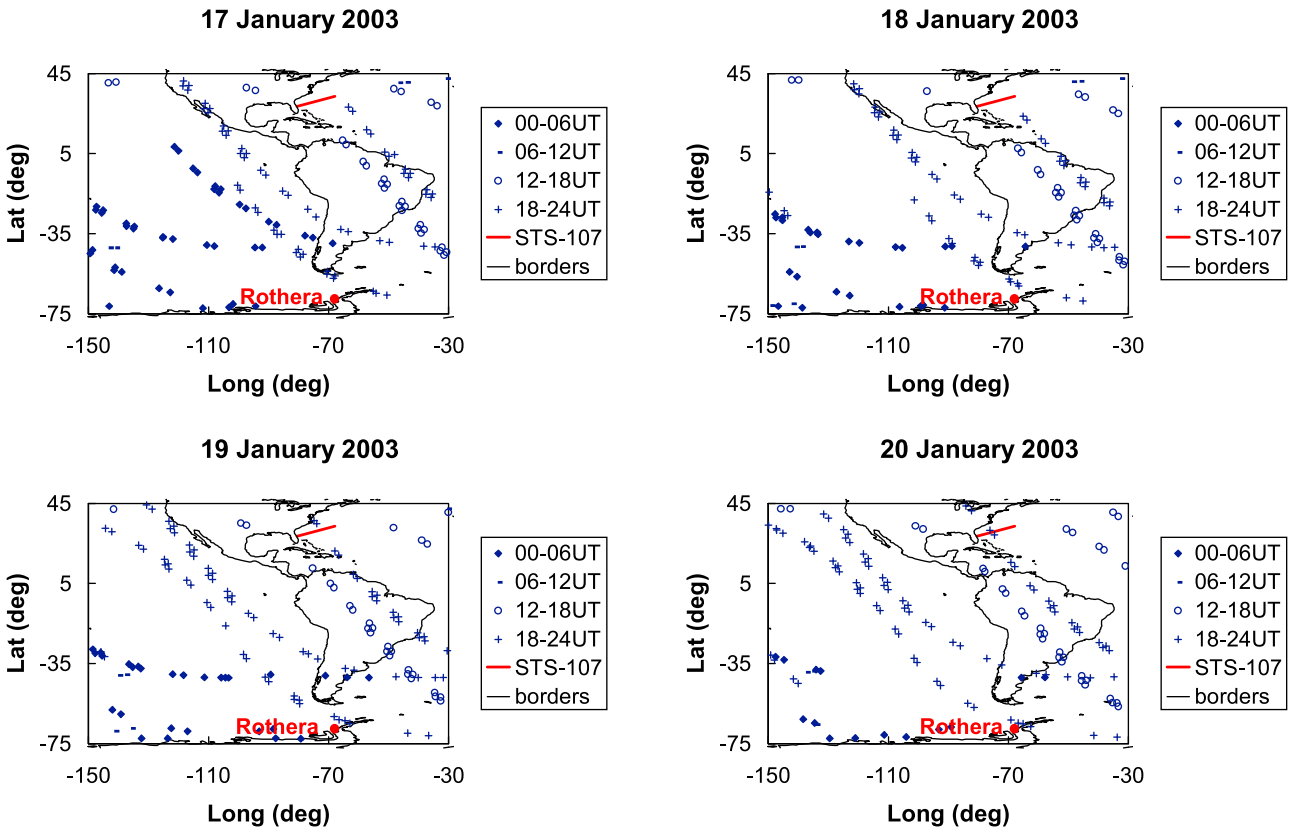

Figure 12. Geo-located positions of all HRDI altitude scans for (top left) 17 January 2003, (top right) 18 January 2003, (bottom left) 19 January 2003 and (bottom right) 20 January 2003. Symbols represent the measurement times of the scans. The red line indicates the shuttle launch ground track.

was viewed along one orbit, and the warm side was viewed during the next. This tended to offset the expected westward progression of limb intercepts due to the orbital revolution of UARS, as illustrated for 17 January 2003: the track crossing the equator at 58°W was acquired by a descending HRDI viewing to the right at 1738 UT, while the track to its east at 50°W longitude was actually acquired later at 1922 UT with HRDI viewing to its left. This leaves a large gap in longitude to the west before the next pair of orbits.

[29] Another difference in reported MLT winds between HRDI and TIDI is the inversion algorithm employed to recover winds. In both cases, the line of sight wind at any altitude is determined from the Doppler shift in the O_2 Atmospheric spectra by calculating the perturbation from a zero-shifted spectrum, that is, when no wind is present. A set of equations is constructed at specific altitude increments (2.5 km) to model an airglow spectrum convolved with a mathematical description of the instrument and an altitude dependent velocity profile. TIDI analysis uses a simple least squares inversion between this set of equations and corresponding measured spectra [*Niciejewski et al.*, 2006] to produce the current Level 2, version 10, product of a line of sight altitude–dependent wind profile at a single geographical point. HRDI analysis uses a sequential estimation technique that assumes that the wind field varies smoothly along the orbital track and employs all measurements, both ahead and behind any specific location, to constrain the wind profile at that location [*Ortland et al.*, 1996]. Both TIDI and HRDI analysis produce a version of the true atmospheric wind profile, though when comparing two profiles acquired within minutes of each other, the HRDI version will show little difference while TIDI retains differences due to random error. The apparent reduction in random error by HRDI is termed an optimal estimate if it is equal to the true geophysical variance and is set by a horizontal smoothing parameter with a constant half-width (in terms of track angle) determined by iteration [*Ortland et al.*, 1996].

[30] Figure 13 displays HRDI meridional wind measurements acquired before, during, and after the 17 January 2003 GUVI observation in Figure 8. Figure 13 (top) brackets the northern end (~40°N) of the shuttle plume at 97°W (1714 UT) and 47°W (1048 UT) and the winds indicate equatorward flow to the east and poleward flow to the west at presumed plume altitudes in the vicinity of 105 km, in conformance with the motion inferred from GUVI imagery. Error bars representing the statistical uncertainty in HRDI winds are shown for the meridional observations corresponding to 97°W. Figure 13 (bottom), acquired when HRDI sampled winds nearer to the equator, suggests strong southward and equator-crossing motion by the meridional wind at plume altitudes. The three profiles acquired at ~1736 UT correspond to single members of the track crossing the equator at 60°W in Figure 12 for 17 January at the listed latitudes. Figure 13 (bottom right) displays members of the track crossing the equator at 50°W at 1912 UT. These HRDI data corroborate the conclusions from both TIDI and GUVI data that the meridional wind can transport shuttle plume exhaust southward from its origin near Florida across the equator. South-

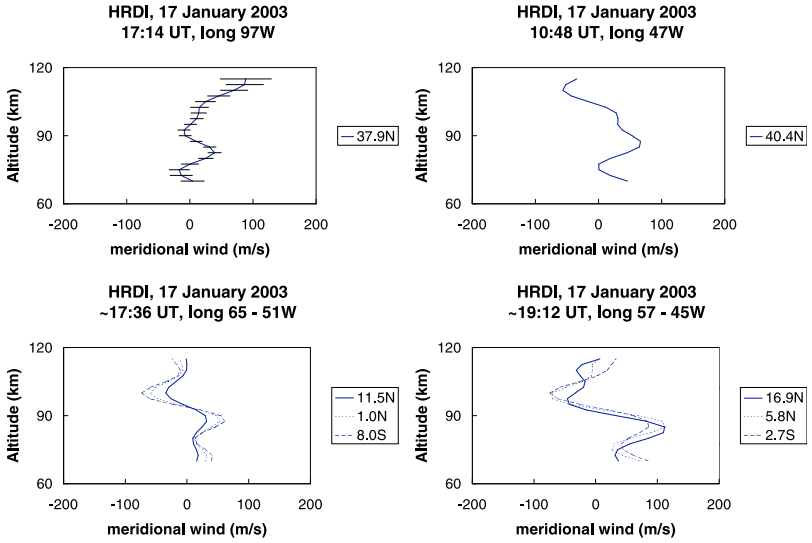

Figure 13. Altitude scans of the meridional wind obtained by HRDI on 17 January 2003. (left) A scan of the (top) northeast section of the plume and equatorial regions acquired ~24 h after launch. (right) Summary of observations at similar latitudes as those in Figure 13 (left) but at different times on different orbits.

ward propagation of the plume dominated the meridional motion from 0339 to 1912 UT on 17 January 2003, at times with a magnitude in excess of 100 m/s.

[31] Southern hemisphere observations by HRDI for the period following the GUVI imagery in Figure 8 and before Figure 11 are shown in Figure 14. Figure 14 (left) was acquired near 2226 UT on 17 January 2003 approximately along the path between the plume images in Figures 8 and 11. There are no distinct SABER H_2O observations of the shuttle plume beyond 24 h after launch to assist in identifying the potential altitude or vertical spread of the shuttle plume. It has been argued that the sudden and dramatic appearance of NLC at high latitudes is related to shuttle launches that occurred a few days prior, and it is generally believed that NLC occur under extremely cold conditions such as the mesopause, which both suggest that shuttle water vapor must descend. A simple linear extrapolation based on the NLC appearance reported by *Kelley et al.* [2009] above Fairbanks, Alaska, at 0919 UT on 11 August 2007 (~60 h following the launch of STS−118), assuming that some portion of the shuttle plume's water vapor content had survived descent and provided nuclei for NLC, suggested a downward progression rate between 5 and 10 km/d depending on the altitude of the display. The meridional flow at 2226 UT on 17 January 2003 was strongly southward along the presumed path of the plume and remained southward at 0310 UT on 18 January 2003 at latitudes in the 30°–40°S range at the presumed western edge of the plume, identified by Figure 11. The zonal flow at the earlier time in Figure 14 suggested a shear in the zonal wind, westerly near the equator and easterly further south, which

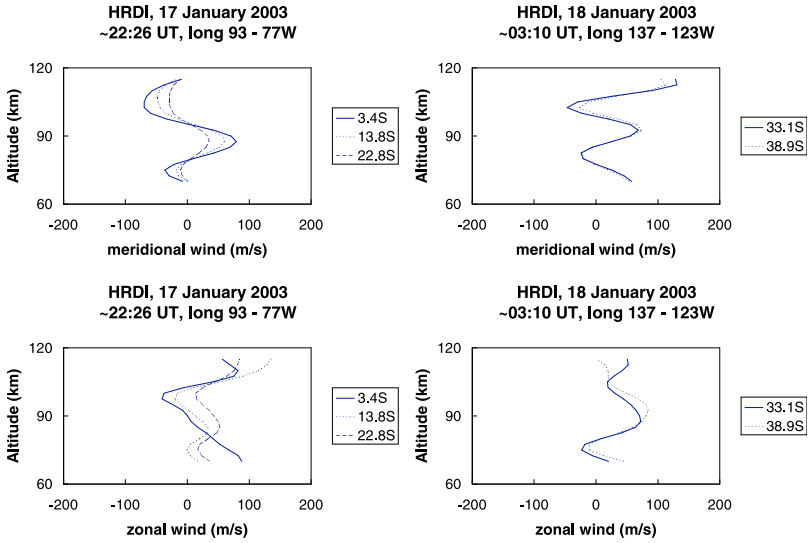

Figure 14. Altitude scans of neutral winds obtained by HRDI approximately 1.5 days after launch in the southern hemisphere along two orbits in the neighborhood of the presumed path of the shuttle plume.

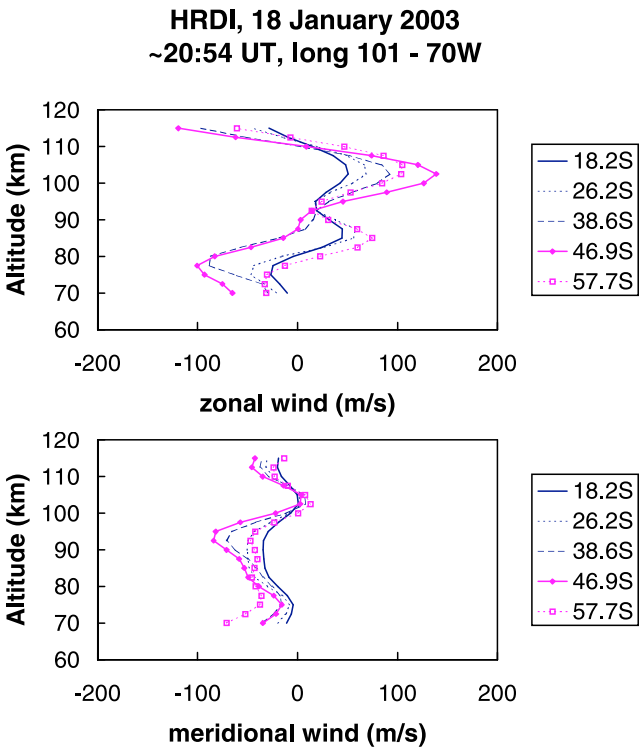

Figure 15. Neutral winds observed by HRDI ~2 days after launch along an orbit that intersects the southern remnants of the shuttle plume.

could disperse some of the plume west, as suggested by Figure 11. The zonal wind was toward the east at the later time in the 30°–40°S band, which could have the effect of containing the plume over the longitudinal range indicated by Figure 11.

[32] The neutral winds in the neighborhood of the GUVI plume were next sampled at ~2054 UT on 18 January 2003 by HRDI, as indicated in Figure 12 along the track (101°W, 18°S to 70°W, 58°S). In Figure 11, the GUVI instrument had just completed orbit 6029 at 1935 UT, crossing the equator near

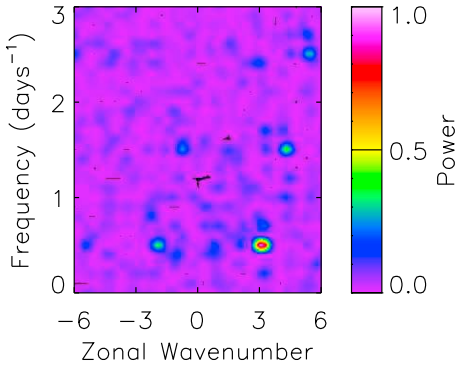

Figure 16. Power spectrum of the meridional wind at 95 km in the latitude range 30°–22.5°S generated from TIDI and HRDI data acquired between 15 and 22 January 2003. The most intense feature corresponds to a 2 day wave (frequency 0.5/day) with wave number 3. The remaining bright features are all aliases of the 2 day wave.

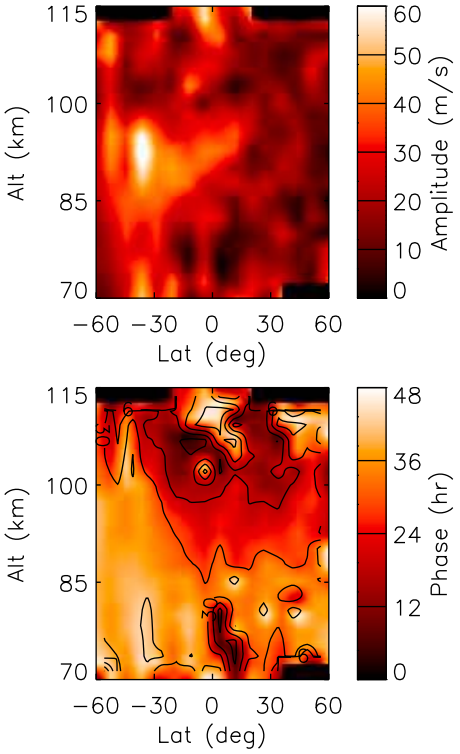

Figure 17. The (top) amplitude and (bottom) phase of a 48 h oscillation with zonal wave number 3 fit to TIDI and HRDI winds acquired between 17 and 19 January 2003 as a function of altitude and latitude. This meridional component suggests a strong 2 day wave peaking at 70 m/s at 40°S in the MLT.

125°W on a path northward after recording the western signature of the exhaust plume at approximately 130°W, 35°S. Altitude profiles of the resolved horizontal components of the neutral wind are displayed in Figure 15. The zonal winds above 90 km are all eastward, while the meridional wind suggests either southward or stagnant flow along the orbital track, depending upon altitude.

[33] Empirical models, such as HWM-07 [*Drob et al.*, 2008], provide a spectral description of neutral winds in the MLT. Short timescale variations are represented by diurnal, semidiurnal, and ter-diurnal variations, which are generally

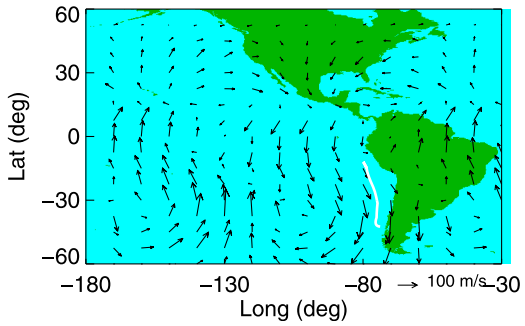

Figure 18. The 2 day wavefield at 1700 UT for 18 January 2003 generated from the least squares fit of TIDI and HRDI winds. The southward path that an air parcel at constant altitude would follow for 24 h ending at the time indicated is shown in white.

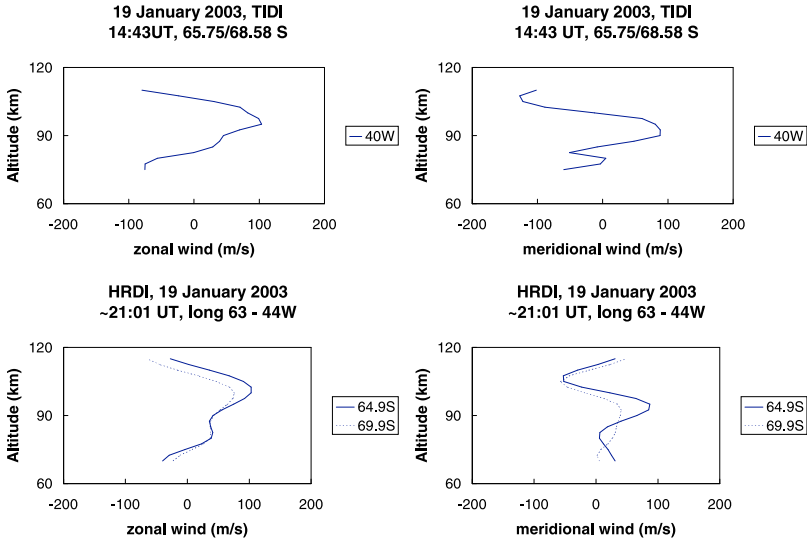

Figure 19. TIDI and HRDI wind profiles acquired over the Antarctic ~3 days after the launch of STS-107.

believed to dominate the MLT wind fields. Both TIMED and UARS perform nearly 15 revolutions of the Earth per day, suggesting that it may be possible to estimate the zonal power spectra of sustained oscillations maintained over several days by transforming wind information in preset latitude bins from (amplitude, longitude, time) to (amplitude, zonal wave number, frequency). TIMED and UARS precess a few degrees per day, which translates to 12 min and 20 min local time per day, respectively, in every latitude bin. In other words, winds acquired over any 10 day stretch by TIDI will correspond to a change in local time of 2 h at any given latitude and over 3 h for HRDI. Some local time coverage is necessary for a power spectral analysis to successfully infer the existence of any sustained atmospheric oscillation by a single satellite, but combining views by two satellites significantly improves the identification process.

[34] *Wu et al.* [1995] describe an elegant method to perform harmonic least squares analysis on irregular data sets such as those collected by TIDI and HRDI. The technique is the space-time analog of time series analysis of unevenly spaced data previously reported by *Scargle* [1982], who demonstrate that a maximum frequency in the periodogram solution is equivalent to the same frequency determined from minimizing the chi square residual in a least squares fit. There is an error in some of the published equations of *Wu et al.* [1995] that did not affect their discussion, their charts, nor the reported absolute values of a follow-on study by *Azeem et al.* [2000]. The corrected equations can be constructed as space-time versions of Appendix C of *Scargle* [1982]. Employing this technique with combined HRDI and TIDI meridional data acquired over the interval 15–22 January 2003 results in a family of power spectra similar to that illustrated in the example of Figure 16. The bright spot at zonal wave number 3 and frequency 0.5/day argues for the existence of a coherent and sustained 2 day wave at 95.0 km altitude over the latitude range 30°S to 22.5°S. All of the other brightly colored spots correspond to aliases due to the limited range of dates used in the analysis. The 2 day wave signature in the meridional flow exists over a wide range of latitude and altitude dominating in power over both the diurnal and semidiurnal signals.

[35] *Wu et al.* [1995] have tabulated the recipe for using the information provided by Figure 16. Since the 2 day signal is so dominant, it is possible to truncate the data length even further in order to reduce temporal variation. *Pancheva et al.* [2006] and *Merkel et al.* [2008] have previously discussed the January 2003 2 day wave. Primarily employing meteor radars, *Pancheva et al.* [2006] have shown the presence of a persistent tropical 2 day wave viewed from Maui on the west, across Brazil to Ascension Island on the east over the time range 1 December 2002 to 28 February 2003. They describe short burst behavior in the amplitude of the 2 day wave lasting several days. *Merkel et al.* [2008] examine SABER temperature data in the second half of a TIMED 60 day yaw cycle, extending from 13 December 2002 to 14 January 2003 and illustrate that a strong 2 day wave exists at 48°S in neutral temperature at 82 km altitude during this 33 day period. Hence, there appears to be unambiguous evidence that the 2 day wave is a significant component of the southern hemisphere dynamical description of the MLT.

[36] A least squares fit of a 48 h periodic oscillation with longitudinal wave number 3 to TIDI and HRDI neutral winds acquired over the period 17–19 January 2003 results in the amplitude/phase model description displayed in Figure 17. A peak amplitude of 70 m/s is determined for 92.5 km altitude at ~40°S latitude in the meridional wind. Note that this is well below the 100 m/s determined above Ascension Island by *Pancheva et al.* [2006], as the fit to the satellite data is representative of a zonally averaged 2 day wave rather than a longitudinally isolated sample. The vector winds displayed in Figure 18 represent the neutral wind field at 1700 UT on 18 January 2003 as determined by this model. A zonal wave number 3 feature implies longitudinal cells of 120 degree width with a positive extent over a range of 60 degrees in longitude. The winds between 60°W and 120°W and between 20°N and 50°S indicate a cell with a clockwise rotation that suggests a path that parcels in the upper atmosphere, such as the STS-107 shuttle plume, could take under the influence of the 2 day wave on 18 January 2003. Such a path, shown as a white line in Figure 18, displays the southward propagation experienced by a parcel under the influence of this modeled

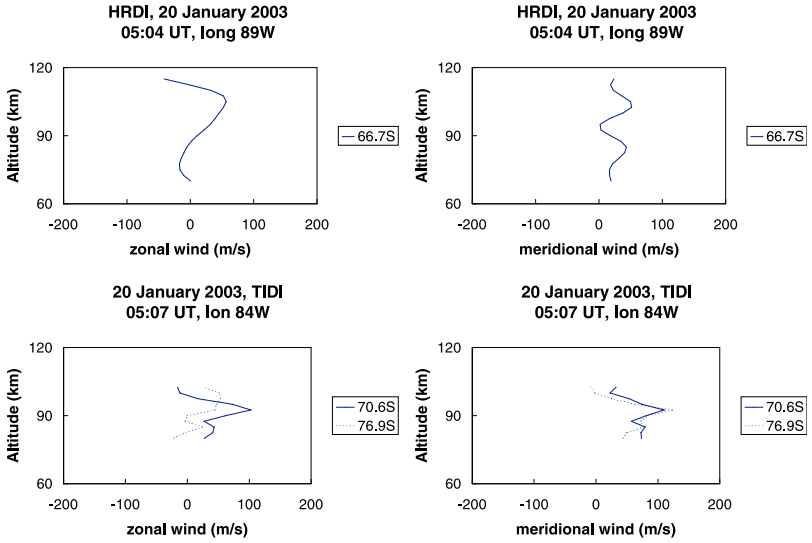

Figure 20. TIDI and HRDI wind profiles acquired over the Antarctic ~3.5 days after the launch of STS-107.

2 day wave for the 24 h period ending at 1700 UT on 18 January 2003. The parcel, beginning in the north at ~12°S travels southward approximately 30 degrees of latitude, or 3000 km in 24 h corresponding to a sustained average speed of 35 m/s solely under the influence of the 2 day wave zonal −average model. Figures 8 and 11 bracket the period of study and provide visible evidence that it is highly probable that the neutral horizontal winds in the MLT associated with this 2 day wave did transport the shuttle plume southward over a vast distance in a short time.

2.5. Observations Near Rothera, 72 h After Launch

[37] A motive of this study was the attempt to understand the registration of several unusual Fe traces above 100 km at Rothera Research Station in the Antarctic (67.6°S, 68°W) between 72 and 88 h following the launch of STS-107. *Stevens et al.* [2005] have argued that since there is no known natural source of Fe at such altitudes, the traces are simply the signatures of iron that has ablated from the shuttle's three main engines during ascent and have been rapidly transported to the Antarctic with the water vapor exhaust. In addition, in the period 3–10 days following launch an unexpected spike in occurrence frequency of polar mesospheric clouds above Rothera was also recorded and directly related to the STS-107 water vapor plume.

[38] Figure 19 describes the resolved neutral horizontal winds observed by TIDI (Figure 19, top) and HRDI (Figure 19, bottom) on 19 January 2003 at roughly coincidental locations near Rothera. The two TIDI line of sight profiles are indicated in Figure 19 (top), while two separate profiles are shown for HRDI and may be collocated using Figure 12. The two independent observations are very similar in character, with the meridional wind near zero at 100 km altitude, poleward above and equatorward below. The zonal flow shows a peak of 100 m/s eastward between 95 and 100 km altitude. A strong echo of Fe was observed at Rothera [*Stevens et al.*, 2005] at 105 km between 1500 and 1600 UT on 19 January 2003, shortly after the TIDI measurement. Two other echoes were recorded later on 20 January 2003, at 110 km near 0100 UT and at 105 km between 0600 and 0800 UT. HRDI and TIDI recorded the horizontal winds displayed in Figure 20 shortly after 0500 UT, the former to the west of Rothera and the latter to the south. Both continue to show an eastward zonal flow and an equatorward flow at presumed plume altitudes. The last successful GUVI image of shuttle effluent acquired a day earlier suggested concentrations to the west which is consistent with the argument that ablated iron in shuttle exhaust was responsible for the Fe traces observed by the Fe resonance lidar above Rothera.

3. Discussion

[39] *Stevens et al.* [2005] argued persuasively for the hypothesis that shuttle exhaust was responsible for two isolated and seemingly unrelated phenomena over the Antarctic Peninsula following the launch of STS-107: unexpected observations of Fe above 100 km and a significant spike in the occurrence frequency of polar mesospheric clouds beginning 3 days after the launch. GUVI Lyman-α imagery indicated the presence and rapid southward propagation of a cloud of enhanced emission, which could have reached Antarctica in time in support of their theory. Their arguments were based upon significant and persistent southward meridional flow inferred from GUVI images that was a factor of five larger than expected from the best climatology.

[40] A summary of the full suite of inferred GUVI meridional winds and measured TIDI and HRDI winds is shown in Figure 21. Figure 21 (top) summarizes the latitude of the plume spread, documented by GUVI, of both the north and south limits, as a function of hours since STS-107 launch. The latitudinal extent of the signatures of Lyman-α emission from the shuttle's exhaust plume from Figures 1, 6, 8, and 11, plus the zero-point and end-point time of the Rothera Fe observations are shown. Figure 21 (bottom) documents the meridional flow inferred from GUVI data, the winds measured by TIDI and HRDI, and the meridional speed determined from the 2 day wave model. The meridional flow inferred from GUVI is simply the mean wind necessary to

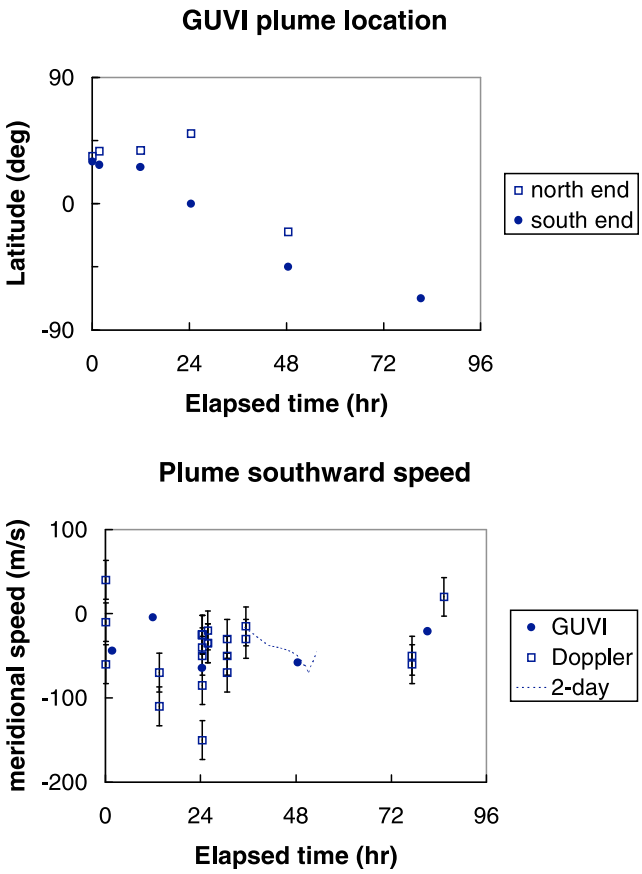

Figure 21. Summary of the transport of the STS-107 plume as observed by GUVI and Doppler wind instruments. (top) Summary of the latitude extent of the plume as a function of elapsed time. The meridional speed of the southern end of the exhaust plume may be inferred from Figure 21 (top). (bottom) The inferred meridional speed from GUVI, the Doppler winds and their uncertainty, and the speed of the modeled 2 day wave along the presumed southerly path of the shuttle plume.

transport the southern edge from one image to the next. There is some uncertainty in these estimates because the hydrogen plume is optically thick, so the edges are difficult to define. As well, because of rapid upward diffusion, hydrogen is spread out vertically and can move differently at different altitudes. The spread in Doppler shift measurements reflects the variability over both latitude and longitude. Note that the winds measured by TIDI at 01 h after launch cover the latitudinal spread indicated by the GUVI image and confirm the inferred motion of the plume: the northern end moved north while the southern end moved south. The winds displayed from the 2 day wave model exhibit a kink at 51 h after launch. This is because the characteristics of the 2 day wave are described independently within each latitude bin and the effects upon the trajectory of a parcel are not smooth when the parcel moves from one 7.5 degree bin to the next. The overall agreement between the inferred southward speed inferred from GUVI and the measured and modeled speeds from TIDI and HRDI is remarkable. Other than at the endpoints, the observations of the motion of the shuttle exhaust plume point to a consistent and sustained southward flow over the 80 h period from launch to the Fe observations above Rothera.

[41] Empirical model descriptions, such as HWM [*Drob et al.*, 2008], identify diurnal and semidiurnal oscillations as the key driving mechanisms for the MLT wind. Indeed, solar influence on the upper atmosphere is the dominant forcing agent of the general long-term behavior in the MLT, and in fact is corroborated by the extensive efforts at identifying the best spectral functions for the sunrise/sunset steps and annual variation used in empirical models. In other words, the mean state and first-order variability of MLT dynamics is best described by current state-of-the-art models that employ oscillatory functions with periods of an integral number of a day and migrate westward with the apparent motion of the sun. It is clear, and models support the inference [*Liu*, 2007, Figure 3a], that a parcel under the influence of a 24 or a 12 h periodic oscillation would return to its initial starting point and not travel very far in the north–south direction in 1 day assuming it is altitude is not changing. Maximum meridional speeds in the MLT region, as output by models, seldom reach or exceed 100 m/s except under geomagnetic forcing at high latitudes. As such, it is difficult to explain the transport of "air" in the MLT over many thousands of kilometers in a period of several days.

[42] First principle physical models describing global circulation in the MLT may be "tuned" to highlight observed phenomena. In a study describing the interaction of a 2 day wave with migrating tides, *Palo et al.* [1998, 1999] tuned subgrid (5° latitude by 5° longitude) processes, including gravity wave effects, to match UARS zonal wind observations of the MLT for December solstice. The geopotential height at the model's lower boundary (35 km) was then modulated with a 160 m amplitude variation consistent with a classical 2 day wave. The model was then run for a constant 15 January. After ~15 days of operation, the winds in the southern hemisphere MLT bore the characteristics of the lower boundary forcing with amplitudes exceeding 80 m/s. In a separate test of a comparable first principle model, *Larsen and Fesen* [2009] investigated various "tunings" with the goal of reproducing large magnitude winds between 95 and 115 km altitude. Surprisingly, agreement between model output and observations was significantly improved by simply changing the vertical resolution of the model. These two examples suggest that the physics incorporated into state-of-the-art numerical models of the general circulation of the MLT are likely sufficient to explain observed features, though the initialization and the operation of the models requires further experimentation.

[43] Corroborating observations are difficult to perform and are few in number. *Larsen* [2002] has collected the most complete summary of sounding rocket chemical release wind profiles through the MLT. These show that maximum winds greater than 100 m/s are observed with a frequency of 60% in the altitude range of 95–115 km. The correspondence with the HWM model, however, is surprisingly accurate in terms of an averaged description: the mean (±1 sigma) meridional and zonal wind profiles deduced from over 400 chemical release experiments essentially envelop all model profiles calculated for the same altitude ranges, observation times, and locations. Only one model calculation approaches 100 m/s, the zonal wind component at 120 km during one flight. The

lesson from this exercise is that climatological averages cannot capture the extreme variability about zero of the neutral wind components.

[44] Planetary waves in the MLT with oscillations whose periods are multiples of a solar day provide an elegant escape from the expectations of climatology and rationalize TIMED and UARS observations. A strong meridional wind can retain southward flow for at least a day and move an air parcel long distances from low to high latitudes, that is, across regions under the influence of different dynamics. Global-scale planetary waves with strong meridional amplitude have been observed previously but are known to be transient. HRDI [*Wu et al.*, 1993, 1994], meteor radars [*Tunbridge and Mitchell*, 2009], and a data assimilation system [*McCormack et al.*, 2010] have documented their seasonal dependence. In the first 21 months of operation of UARS, HRDI recorded strong 2 day wave events in the southern hemisphere for January in both 1992 and 1993. It is not surprising then to observe a strong 2 day wave in January of 2003 coincident with the launch of STS-107.

[45] The ability to observe and confirm the meridional component of the 2 day wave from orbit by two completely independent satellites viewing the Doppler shift of the O_2 airglow in the terrestrial limb is compelling. The daily precession of each satellite is extremely limiting, implying the local solar time observed along an orbital track is duplicated along all 15 daily orbital tracks. Hence, the space-time dependence of any spectral signature in the neutral wind cannot be easily determined without additional assumptions, such as vertical wavelength. Including observations from another instrument, viewing along an orbital track with a completely different local time reduces the ambiguity or alias in assigning a spectral signature. Only when employing both TIDI and HRDI observations, can it be shown that the 2 day wave is dominant on the day of the shuttle launch. And only if the 2 day wave is dominant, can the hypothesis that shuttle exhaust can be transported from Florida to the Antarctic in 80 h be made. It is unfortunate that TIMED was not a two-satellite mission as originally intended [*Yee et al.*, 1999] and fortunate that UARS attitude corrections could be made successfully restoring the utility of HRDI.

[46] *Kelley et al.* [2009] have postulated an alternate explanation for rapid poleward transfer of shuttle plume exhaust for the 7 August 2007 launch of STS-119 and for the presumed rapid zonal transport of ejecta from the "Great Siberian Impact Event" of 30 June 1908. In both cases, unexpected and bright nocturnal clouds appeared shortly after each event, identified as noctilucent clouds for the former and cirrostratus plus cirrus for the latter. The hypothesis proposed by *Kelley et al.* [2009] is based on a pair of simultaneous wind profile observations performed by *Larsen and Odom* [1997] with a separation of 450 km at the magnetic equator along the northeastern coast of Brazil in September 1994. Neutral winds measured below 140 km altitude were markedly different between the two profiles with strong southward winds observed at the northern launch site and stronger eastward winds at the equator. *Kelley et al.* [2009] suggest that the difference in the winds over the 450 km horizontal range between the two sites is the source for quasi-two-dimensional (Q-2-D) turbulence in the mesoscale regime. Assuming horizontal wind fluctuations in the MLT exist during the launch of STS-119 as well as during the Tunguska event and invoking Q-2-D turbulence, energy could be transferred from the small-scale plume phenomena (or other coexisting structure) to the synoptic neutral wind field thereby transporting water vapor rapidly over large distances. *Kelley et al.* [2009] correctly indicate that there is a lack of experimental and theoretical development of their hypothesis for thermospheric altitudes, but there are simple alternative explanations for horizontal wind gradients at mesoscale distances. Significant efforts at describing similar observations at lower altitudes beginning with *Dewan* [1979], suggest that gravity waves cannot be ruled out as a viable alternative. *Cho et al.* [1999] examine the horizontal wave number spectra of horizontal neutral winds collected from aircraft flying between 2 and 12 km in a concerted diagnostic effort to differentiate whether Q-2-D, gravity waves, or vortical modes dominate mesoscale atmospheric fluctuations, and appear to observe all three effects depending on latitude and scale lengths. *Lindborg* [2007] argue against gravity waves, but find that the energy flux is directed from large-scale to small-scale sizes in the mesoscale range. Recent satellite observations of temperature and water vapor altitude profiles [*Kahn and Teixeira*, 2009] indicate a complex interplay between latitude, season, and altitude at horizontal mesoscale lengths related to the transfer of energy across scales. Rather than invoking an untested and uncertain hypothesis to explain strong and sustained meridional winds in the MLT, we have shown that the appearance of high-altitude Fe above Rothera Station, Antarctica, may simply be explained by entrainment of iron from the ablation of the main engines of STS-107 with the water vapor exhaust plume, were constrained to flow southward by an intense 2 day wave in the southern hemisphere. We cannot preclude the mechanism suggested by *Kelley et al.* [2009] for plume transport in the thermosphere, but show that it is not needed.

[47] The TIDI and HRDI Doppler shift measurements, carefully described in chronological order above, are consistent with and fully support the assertions of *Stevens et al.* [2005]. The analysis has only recently become possible due to important improvements in the instrumental characterization and understanding of both instruments that were unavailable at the time of previous publications. The fact that the Doppler shift measurements verify the inferred speeds extracted from GUVI imagery might also be turned around: the GUVI images of a long lasting "chemical release" experiment verify the accuracy of TIDI and HRDI Doppler wind measurements, in particular, the recent improvements in retrieval and inversion algorithms and instrument description. The value of a long-lasting chemical release experiment lies in validating the zero wind position of the instrument monitoring the Doppler shift. Statistical uncertainties in the Level 1 line of sight winds reported by TIDI and HRDI are generally between 5 and 10 m/s under most circumstances, though there is a strong dependence upon count rate (airglow brightness). The systematic offset in line of sight winds due to poor knowledge of absolute zero wind, the rest position of the emission spectrum recorded by the Doppler spectrometer, is more difficult to determine and report and requires nearly perfect knowledge of both instrumental artifacts and satellite pointing (attitude). *Burrage et al.* [1993, 1996] carefully document extensive wind calibration efforts and procedures for HRDI, some of which have also been used for TIDI. The use of a long-lived tracer as a verification of spaceborne

Doppler wind measurements has never been sought. Long-lived tracers were at one time thought to be an elegant method to document atmospheric dynamics: twilight photometric observations of lithium over the Antarctic, coincident with high-altitude atmospheric detonation of nuclear explosives at Johnson Atoll in 1958 implied a southward meridional speed of 30 m/s, suggesting the injection of rare alkali metals at high altitudes as a tracer of upper atmospheric winds [*Vallance Jones*, 1963]. The cross-calibration available with GUVI Lyman-α imagery of shuttle launches, as suggested above, will be a topic of further investigation.

4. Conclusions

[48] Significant progress in understanding the instrumental artifacts presented by satellite issues on HRDI and TIDI (loss of attitude knowledge, deposition of outgassing products onto the optical path) has matured and improved their Doppler wind products. In the latter stages of their respective missions, verification studies must rely upon good fortune. The successful verification of documented but unexplained rapid transit of a space shuttle exhaust plume from launch off the Florida coast to the Antarctic with HRDI and TIDI indicates high confidence in their respective products. This study has demonstrated:

[49] 1. Apparently high and anomalous meridional winds, inferred from satellite based imagery are real and may be explained by invoking a 2 day planetary wave, strongest in the southern hemisphere.

[50] 2. Displacement of the plume 1 h removed from the original injection site is consistent with Doppler shifts measured in the vicinity of the launch ground track.

[51] 3. Meridional winds measured with Doppler shifts of airglow spectra coincide with both northwestern shifts of the northernmost end of the shuttle plume and southerly shifts of the southernmost end evident 24 h after launch.

[52] 4. A classical 2 day wave with a zonal wave number of 3 contains the zonal distribution of the shuttle exhaust plume within a 60 degree swath at southerly latitudes inferred from meridional motion 48 h after launch.

[53] 5. Weaker zonal winds are consistent with transporting plume material over Rothera, Antarctica 80 h after launch from the eastern United States.

[54] 6. Altitude profiles from infrared H_2O and OH spectra suggest descent rates of the shuttle plume that are consistent with populating the upper mesosphere with vapor to form clouds.

[55] 7. TIDI wind profiles from the start of the TIMED mission provide an accurate description of MLT neutral winds.

[56] 8. A global tidal description of the MLT on the time frame of a few days is possible when two satellites provide independent limb scan neutral wind profiles at unrelated LST (local solar times).

[57] 9. Strong (>100 m/s) magnitude winds in the MLT, appearing to be outliers statistically in individual profiles, are as common in satellite Doppler observations as they are in "chemical tracer" experiments, due to the high SNR observations of limb airglow spectra which negates the need for spatial and temporal averaging that are a necessity in classical ground-based RF and lidar techniques.

[58] Future studies of neutral winds measured by HRDI and TIDI that coincide with other observations of shuttle induced high-altitude polar clouds at solstice will address the newly discovered importance of planetary waves in transporting air parcels long distances in the MLT. The coincident data set encompass the period from February 2002 to March 2005. If 100 m/s winds and strong wind shears are as common in the MLT as inferred from sounding rocket chemical release tracer experiments and satellite Doppler observations, then it is important that operational models that forecast MLT dynamics incorporate the proper parameterization in order to better predict large-scale transport patterns.

[59] **Acknowledgments.** The authors wish to thank the SABER and GUVI Science and Data Processing teams for their careful processing, analysis, and validation of their data. This research was supported by NASA contracts NNX07AB72G and NNH09ZDA001N. One of us (R.N.) gratefully acknowledges support from ASEE and the 2005 ONR Summer Faculty Research Program for providing the initial funding for this study. R.R.M. and M.H.S. thank the NASA Guest Investigator Program for support.

[60] Robert Lysak thanks the reviewers for their assistance in evaluating this paper.

References

Azeem, S. M. I., T. L. Killeen, R. M. Johnson, Q. Wu, and D. A. Gell (2000), Space-time analysis of TIMED Doppler Interferometer (TIDI) measurements, *Geophys. Res. Lett.*, *27*, 3297, doi:10.1029/1999GL011289.

Burrage, M. D., et al. (1993), Comparison of HRDI wind measurements with radar and rocket observations, *Geophys. Res. Lett.*, *20*, 1259, doi:10.1029/93GL01108.

Burrage, M. D., et al. (1996), Validation of mesosphere and lower thermosphere winds from the high resolution Doppler imager on UARS, *J. Geophys. Res.*, *101*, 10,365, doi:10.1029/95JD01700.

Cho, J. Y. N., R. E. Newell, and J. D. Barrick (1999), Horizontal wavenumber spectra of winds, temperature, and trace gases during the Pacific Exploratory Missions: 2. Gravity waves, quasi-two-dimensional turbulence, and vortical modes, *J. Geophys. Res.*, *104*, 16,297, doi:10.1029/1999JD900068.

Dewan, E. M. (1979), Stratospheric wave spectra resembling turbulence, *Science*, *204*, 832, doi:10.1126/science.204.4395.832.

Drob, D. P., et al. (2008), An empirical model of the Earth's horizontal wind fields: HWM07, *J. Geophys. Res.*, *113*, A12304, doi:10.1029/2008JA013668.

Fisher, G. M., R. J. Niciejewski, T. L. Killeen, W. A. Gault, G. G. Shepherd, S. Brown, and Q. Wu (2002), Twelve-hour tides in the winter northern polar mesosphere and lower thermosphere, *J. Geophys. Res.*, *107*(A8), 1211, doi:10.1029/2001JA000294.

Hedin, A. E., et al. (1991), Revised global model of thermosphere winds using satellite and ground-based observations, *J. Geophys. Res.*, *96*, 7657, doi:10.1029/91JA00251.

Hicks, G. T., T. A. Chubb, and R. R. Meier (1999), Observations of hydrogen Lyman α emission from missile trails, *J. Geophys. Res.*, *104*, 10,101, doi:10.1029/1999JA900029.

Kahn, B. H., and J. Teixeira (2009), A global climatology of temperature and water vapor variance scaling from the Atmospheric Infrared Sounder, *J. Clim.*, *22*, 558, doi:10.1175/2009JCLI2934.1.

Kelley, M. C., C. E. Seyler, and M. F. Larsen (2009), Two-dimensional turbulence, space shuttle plume transport in the thermosphere, and a possible relation to the Great Siberian Impact Event, *Geophys. Res. Lett.*, *36*, L14103, doi:10.1029/2009GL038362.

Kelley, M. C., M. J. Nicolls, R. H. Varney, R. L. Collins, R. Doe, J. M. C. Plane, J. Thayer, M. Taylor, B. Thurairajah, and K. Mizutani (2010), Radar, lidar, and optical observations in the polar summer mesosphere shortly after a space shuttle launch, *J. Geophys. Res.*, *115*, A05304, doi:10.1029/2009JA014938.

Kellogg, W. W. (1964), Pollution of the upper atmosphere by rockets, *Space Sci. Rev.*, *3*, 275, doi:10.1007/BF00180267.

Larsen, M. F. (2002), Winds and shears in the mesosphere and lower thermosphere: Results from four decades of chemical release wind measurements, *J. Geophys. Res.*, *107*(A8), 1215, doi:10.1029/2001JA000218.

Larsen, M. F., and C. G. Fesen (2009), Accuracy issues of the existing thermospheric wind models: Can we rely on them in seeking solutions to

wind-driven problems?, *Ann. Geophys.*, *27*, 2277, doi:10.5194/angeo-27-277-2009.

Larsen, M. F., and C. D. Odom (1997), Observations of altitudinal and latitudinal *E* region neutral wind gradients near sunset at the magnetic equator, *Geophys. Res. Lett.*, *24*, 1711, doi:10.1029/97GL01469.

Lindborg, E. (2007), Horizontal wavenumber spectra of vertical vorticity and horizontal divergence in the upper troposphere and lower stratosphere, *J. Atmos. Sci.*, *64*, 1017, doi:10.1175/JAS3864.1.

Liu, H.-L. (2007), On the large wind shear and fast meridional transport above the mesopause, *Geophys. Res. Lett.*, *34*, L08815, doi:10.1029/2006GL028789.

McCormack, J. P., S. D. Eckermann, K. W. Hoppel, and R. A. Vincent (2010), Amplification of the quas-two day wave through nonlinear interaction with the migrating diurnal tide, *Geophys. Res. Lett.*, *37*, L16810, doi:10.1029/2010GL043906.

Meier, R. R., J. M. C. Plane, M. H. Stevens, L. J. Paxton, A. B. Christensen, and G. Crowley (2010), Can molecular diffusion explain Space Shuttle plume spreading?, *Geophys. Res. Lett.*, *37*, L08101, doi:10.1029/2010GL042868.

Mendillo, M., B. Herniter, and D. Rote (1980), Modification of the aerospace environment by large space vehicles, *J. Spacecr. Rockets*, *17*, 226, doi:10.2514/3.57731.

Meriwether, J. W., and A. J. Gerrard (2004), Mesosphere inversion layers and stratosphere temperature enhancements, *Rev. Geophys.*, *42*, RG3003, doi:10.1029/2003RG000133.

Merkel, A. W., R. R. Garcia, S. M. Bailey, and J. M. Russell III (2008), Observational studies of planetary waves in PMCs and mesospheric temperature measured by SNOE and SABER, *J. Geophys. Res.*, *113*, D14202, doi:10.1029/2007JD009396.

Niciejewski, R. J., and T. L. Killeen (1995), Nocturnal observations of the semidiurnal tide at a midlatitude site, *J. Geophys. Res.*, *100*, 25,855, doi:10.1029/95JD02729.

Niciejewski, R., Q. Wu, W. Skinner, D. Gell, M. Cooper, A. Marshall, T. Killeen, S. Solomon, and D. Ortland (2006), TIMED Doppler Interferometer on the Thermosphere Ionosphere Mesosphere Energetics and Dynamics satellite: Data product overview, *J. Geophys. Res.*, *111*, A11S90, doi:10.1029/2005JA011513.

Oppenheim, M. M., G. Sugar, N. O. Slowey, E. Bass, J. L. Chau, and S. Close (2009), Remote sensing lower thermosphere wind profiles using non-specular meteor echoes, *Geophys. Res. Lett.*, *36*, L09817, doi:10.1029/2009GL037353.

Ortland, D. A., W. R. Skinner, P. B. Hays, M. D. Burrage, R. S. Lieberman, A. R. Marshall, and D. A. Gell (1996), Measurements of stratospheric winds by the high resolution Doppler imager, *J. Geophys. Res.*, *101*, 10,351, doi:10.1029/95JD02142.

Palo, S. E., R. G. Roble, and M. E. Hagan (1998), TIME-GCM results for the quasi-two-day wave, *Geophys. Res. Lett.*, *25*, 3783, doi:10.1029/1998GL900032.

Palo, S. E., R. G. Roble, and M. E. Hagan (1999), Middle atmosphere effects of the quasi-two-day wave determined from a general circulation model, *Earth Planets Space*, *51*, 629.

Pancheva, D. V., et al. (2006), Two-day wave coupling of the low-latitude atmosphere-ionosphere system, *J. Geophys. Res.*, *111*, A07313, doi:10.1029/2005JA011562.

Scargle, J. D. (1982), Studies in astronomical time series analysis. II. Statistical aspects of spectral analysis of unevenly spaced data, *Astrophys. J.*, *263*, 835, doi:10.1086/160554.

Siskind, D. E., M. H. Stevens, J. T. Emmert, D. P. Drob, A. J. Kochenash, J. M. Russell III, L. L. Gordley, and M. G. Mlynczak (2003), Signatures of shuttle and rocket exhaust plumes in TIMED/SABER radiance data, *Geophys. Res. Lett.*, *30*(15), 1819, doi:10.1029/2003GL017627.

Skinner, W. R., A. R. Marshall, D. A. Gell, and J. Raines (2003), The High Resolution Doppler Imager: Status update 12 years after launch, *Proc. SPIE*, *5157*, 231, doi:10.1117/12.504563.

Stevens, M. H., C. R. Englert, and J. Gumbel (2002), OH observations of space shuttle exhaust, *Geophys. Res. Lett.*, *29*(10), 1378, doi:10.1029/2002GL015079.

Stevens, M. H., J. Gumbel, C. R. Englert, K. U. Grossmann, M. Rapp, and P. Hartogh (2003), Polar mesospheric clouds formed from space shuttle exhaust, *Geophys. Res. Lett.*, *30*(10), 1546, doi:10.1029/2003GL017249.

Stevens, M. H., R. R. Meier, X. Chu, M. T. DeLand, and J. M. C. Plane (2005), Antarctic mesospheric clouds formed from space shuttle exhaust, *Geophys. Res. Lett.*, *32*, L13810, doi:10.1029/2005GL023054.

Tansock, J. J., et al. (2003), SABER ground calibration, *Int. J. Remote Sens.*, *24*, 403, doi:10.1080/01431160304969.

Tunbridge, V. M., and N. J. Mitchell (2009), The two-day wave in the Antarctic and Arctic mesosphere and lower thermosphere, *Atmos. Chem. Phys.*, *9*, 6377, doi:10.5194/acp-9-6377-2009.

Vallance Jones, A. (1963), Metallic emissions in the twilight and their bearing on atmospheric dynamics, *Planet. Space Sci.*, *10*, 117, doi:10.1016/0032-0633(63)90012-6.

Winick, J. R., P. P. Wintersteiner, R. H. Picard, D. Esplin, M. G. Mlynczak, J. M. Russell III, and L. L. Gordley (2009), OH layer characteristics during unusual boreal winters of 2004 and 2006, *J. Geophys. Res.*, *114*, A02303, doi:10.1029/2008JA013688.

Wu, D. L., P. B. Hays, W. R. Skinner, A. R. Marshall, M. D. Burrage, R. S. Lieberman, and D. A. Ortland (1993), Observations of the quasi 2-day wave from the high resolution Doppler imager on UARS, *Geophys. Res. Lett.*, *20*, 2853, doi:10.1029/93GL03008.

Wu, D. L., P. B. Hays, and W. R. Skinner (1994), Observations of the 5-day wave in the mesosphere and lower thermosphere, *Geophys. Res. Lett.*, *21*, 2733, doi:10.1029/94GL02660.

Wu, D. L., P. B. Hays, and W. R. Skinner (1995), A least squares method for spectral analysis of space-time series, *J. Atmos. Sci.*, *52*, 3501, doi:10.1175/1520-0469(1995)052<3501:ALSMFS>2.0.CO;2.

Yau, A. W., B. A. Whalen, F. Creutzberg, M. B. Pongratz, and G. Smith (1981), Observations of particle precipitation, electric field, and optical morphology of an artificially perturbed auroral arc: Project Waterhole, *J. Geophys. Res.*, *86*, 5601, doi:10.1029/JA086iA07p05601.

Yee, J.-H., G. E. Cameron, and D. Y. Kusnierkiewicz (1999), An overview of TIMED, *Proc. SPIE*, *3756*, 244, doi:10.1117/12.366378.

M. Cooper, A. Marshall, R. Niciejewski, and W. Skinner, Space Physics Research Laboratory, University of Michigan, Ann Arbor, MI 48109, USA. (niciejew@umich.edu)

R. R. Meier, Department of Physics and Astronomy, George Mason University, Fairfax, VA 22030, USA.

D. Ortland, NorthWest Research Associates, PO Box 3027, Bellevue, WA 98009, USA.

M. H. Stevens, Space Science Division, Naval Research Laboratory, Washington, DC 20375, USA.

Q. Wu, National Center for Atmospheric Research, Boulder, CO 80307, USA.